34th Annual International Conference of the IEEE EMBS
San Diego, California USA, 28 August - 1 September, 2012

Adaptive Pulse Segmentation and Artifact Detection in Photoplethysmography for Mobile Applications

Walter Karlen[1], *Member, IEEE,* J. Mark Ansermino[1], and Guy Dumont[1] *Fellow, IEEE*

Abstract— **Pulse oximeters non-invasively measure heart rate and oxygen saturation and have great potential for predicting critical illness. The photoplethysmogram (PPG) recorded from pulse oximetry is often corrupted with artifacts. These artifacts render the derived vital signs inaccurate.**

We present a novel real-time algorithm for segmentation of the PPG into pulses and for the classification of artifacts. The Incremental-Merge Segmentation (IMS) algorithm operates in the time domain and extracts morphological features of the PPG. These features are line segments that are classified as pulses or artifacts using adaptive thresholds.

The IMS algorithm was evaluated using the Complex System Laboratory (CSL) Benchmark dataset. A sensitivity of 98.93% and positive predictive value of 96.68% have been obtained, which compares very favorably with the CSL benchmark algorithm. The novel algorithm is currently being implemented into mobile phone pulse oximeters.

I. Introduction

Pulse oximeters offer a non-invasive measurement of the photoplethysmogram (PPG) from which heart rate and oxygen saturation (SpO_2) is derived. Respiratory rate can also be estimated from the PPG [1]. SpO_2, heart rate, and respiratory rate are predictors of critical illness, such as sepsis, pneumonia and pre-eclampsia, whose outcome is more severe in remote and resource poor areas. The non-invasive measurement of these vital signs with a single device like the pulse oximeter would provide an ideal solution for diagnosis and monitoring of diseases. However, current clinical pulse oximeter monitors are not tailored to perform spot check diagnostics, do not provide respiratory rate calculations, and their bulk, high-cost, and poor user interfaces prevent widespread adoption in resource poor areas.

Pulse oximeters use two light emitting diodes (LEDs) that actively illuminate the patient's tissue (usually at the finger tip) alternately at two different wavelengths (red and infrared). The intensity of the non-absorbed light at each wavelength is measured with a photodiode. The light absorption and transmission depends on the traveled light path, optical density of the tissue, volume of blood present in the tissue, and blood composition [2]. This allows the display of the variation of blood volume over time in the finger resulting in a PPG. While oxygenated hemoglobin absorbs more infrared light and allows more red light to pass through the tissue, deoxygenated hemoglobin allows more infrared light to pass and absorbs more red. This property of hemoglobin allows for SpO_2 estimation.

Combined with a pulse oximeter, the inherent capabilities of a standard mobile phone have the potential to overcome the limitations of a standalone pulse oximeter, and enable the intelligent analysis and intuitive communication of information to a health care worker. The low-cost technology of mobile phones is readily available in low income countries and offers computing capabilities for biomedical signal processing and decision making. In addition, the battery power of mobile phones guarantees portability and usage in remote areas that are not connected to the power grid. This same feature, however, also challenges the engineer to maximize available resources. We have previously demonstrated the Phone Oximeter, a mobile phone application that connects a high-end pulse oximeter to a mobile phone, as an intuitive tool for the operating room [3]. We are now working towards low-cost pulse oximeter solutions adapted for the diagnosis of global diseases. With the aim of developing power efficient signal processing algorithms for the calculation of vital signs with a pulse oximeter on mobile phones, we present our recent algorithm developments for robust beat and artifact detection in the PPG.

A. Background

The raw PPG waveform is characterized by an AC component that corresponds to the heart beat induced variation of blood volume in the arteries and a DC component that corresponds to the constant amount of absorption from predominantly tissues and non-pulsatile venous blood. Only the AC component is relevant for the extraction of the heart beat. However, artifacts can be recognized in both the AC and DC components (Fig. 1). Artifacts are frequently accompanied by a large rapid fluctuation of the DC component. Unfortunately, most commercial pulse oximeter devices provide only a band-pass filtered and/or auto-scaled PPG signal where the original DC component has been eliminated and is not visible to the user. In these heavily filtered situations the PPG signal frequently becomes saturated and clipped due to artifacts and baseline shifts (Fig. 1).

B. Previous Work

A wide range of algorithms have been suggested to detect pulses and to detect or eliminate artifacts in PPG signals. Many algorithms segment the PPG. The segmentation is mainly done using the derivative of the PPG signal [4], [5]. Other approaches include multi-stage band-pass filters [6] or adaptive frequency estimators [7]. In addition, to

This work was supported by the Swiss National Science Foundation.

[1]W. Karlen, J.M. Ansermino and G. Dumont are with the Electrical & Computer Engineering in Medicine Group, Departments of Electrical & Computer Engineering and Anesthesiology, Pharmacology & Therapeutics, The University of British Columbia (UBC), 2332 Main Mall, Vancouver, BC, V6T 1Z4, Canada. Contact: walter.karlen@ieee.org

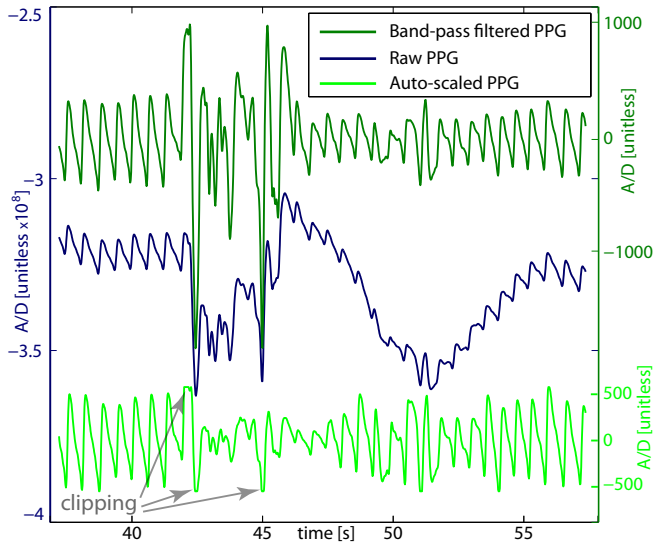

Fig. 1. PPG signal at different processing stages corrupted by artifacts. With auto-scaled signals, clipping occurs during artifacts and large baseline shifts.

limit errors, physiological limits for heart rate are taken into account [5]–[7]. Artifacts are detected by comparing the morphology of the PPG beats to thresholds [8] or a cross-correlation is performed with a template waveform [4]. Corrupted PPGs have been identified using Independent Component Analysis [9]. All these methods are relatively computationally intensive and not well suited for a mobile device. Our aim was to develop an accurate real-time beat and artifact detection algorithm for PPG signals that operates in the time domain, requires low processing power and is ready to be implemented in a battery-powered mobile device.

II. Algorithm Description

The periodic component must be extracted from the PPG signal to perform automated heart rate and artifact detection. The regular heart beat pulsations are characterized by a maximal volume peak, sometimes followed by a secondary peak called the dicrotic notch. The waveform is processed with a line segmentation algorithm that segments the PPG into pulses. Since PPG pulse components are based on a morphological shape that can be characterized by consecutive lines, this algorithm permits the desired trend calculation in an efficient manner. Segments can be easily identified and compared. Mismatching segments indicate potential artifacts.

A. Preprocessing

No other filtering than the standard band-pass filter applied by pulse oximeter manufacturers to remove the DC component of the PPG signal is necessary.

B. Line Segmentation

The proposed Incremental-Merge Segmentation (IMS) method (Algorithm 1) is a mixture of Iterative-End-Point-Fit [10] and Incremental algorithms [11] that were originally developed for computer vision and mobile robotics applications. A similar approach has also been used for

Algorithm 1 Incremental-Merge Segmentation algorithm

$seg \leftarrow 1; z \leftarrow 1;\ segInLine \leftarrow 1$
$line_z \leftarrow constructLine([p_{seg}, p_{seg+m}])$
$z \leftarrow z+1; seg \leftarrow seg+1$
loop
  $line_z \leftarrow constructLine([p_{seg\times m}, p_{(seg+1)*m}])$
  if α_z & α_{z-1} have the same sign **then** ▷ merge
    $line_{z-1} \leftarrow$
    $constructLine([p_{(seg-segInLine)\times m}, p_{(seg+1)*m}])$
    $seg \leftarrow seg+1$
    $segInLine \leftarrow segInLine+1$
  else ▷ start new segment
    $z \leftarrow z+1$
    $seg \leftarrow seg+1$
    $segInLine \leftarrow 1$
  end if
end loop

Where $m+1$ is the size of a line segment, p_n is the nth point of the time series, z is the counter for lines, seg is the counter for segments, α_z is the slope of line z, and $segInLine$ is the counter for line segments in a constructed line.

the compression of ECG signals with segmentation [12]. Because of its sliding-window structure, the IMS algorithm is simple, fast and can be executed in real-time. The tuning of the algorithm requires the setting of only one parameter m (length of line segments in number of sample points minus one), which is dependent on the sampling rate. Line segments are constructed by connecting the first and last points of the line (End-Point-Fit). After the slopes of these lines are computed, consecutive lines with matching slopes are incrementally combined. If the slopes do not match, a new segment is constructed.

C. Line Classification

After a line segment is finalized it is classified. Lines falling within an amplitude range between ThA_{high} and ThA_{low} or larger than duration $ThT = 0.03$ s are classified as 1) an up-slope, 2) a down-slope, or 3) a horizontal line. To prevent misdetection of the dicrotic notch and artifacts as individual pulses, the amplitude thresholds $ThA_{high,low}$ are calculated adaptively as described in Algorithm 2.

Pulse peaks are identified as endpoints of the validated up-slopes. The obtained features are amplitude of pulse, maximum and minimum intensity of each pulse, and pulse period which are also used for artifact detection.

D. Artifact Detection

Corruption of the PPG signal because of movement artifacts or sensor disconnection is detected online by comparing consecutive line amplitudes and intervals. Up-slopes preceding and succeeding a horizontal line (clipping or disconnection) are automatically labeled as artifacts (Fig. 2). Further, up-slopes with amplitudes exceeding the adaptive upper threshold ThA_{high} are labeled as artifacts. Interbeat-interval limitation is taken into account. Beats with less than

Algorithm 2 Adaptive threshold algorithm

$ThA_{low} \leftarrow \theta_1 \times 0.6$ ▷ init thresholds
$ThA_{high} \leftarrow \theta_1 \times 1.4$
loop
  if $\alpha_z > 0$ & $\alpha_{z-1} \neq 0$ & $\alpha_{z+1} \neq 0$ **then**
    if $\theta_z \geq ThA_{low}$ & $\theta_z \leq ThA_{high}$ **then**
      $ThA_{low} \leftarrow (ThA_{low} + \theta_z \times a_{fast}^{low})/2$
      $ThA_{high} \leftarrow \theta_z \times a_{fast}^{high}$
      $\lambda \leftarrow 0$
    else
      if $\lambda > 0$ **then** ▷ delay adaptation
        $Th_{low} \leftarrow (ThA_{low} + \theta_{seg} \times a_{slow}^{low})/2$
        $ThA_{high} \leftarrow \theta_z \times a_{slow}^{high}$
      end if
      $\lambda \leftarrow \lambda + 1$ ▷ increment flag
    end if
  end if
  $z \leftarrow z + 1$ ▷ increment line counter
end loop

Where a_x^y are the adaptation parameters, z is the counter for lines, α_z is the slope, and θ_z is the amplitude of line z.

50% of the previous valid interbeat-interval or less than the physiological limit of 240 ms (250 bpm) are labeled by the algorithm as artifacts.

III. Experiments

For algorithm development and calibration, we used the inVivo CapnoBase (CB) dataset [13]. Following institutional review board approval, data was gathered from 59 children and 35 adults receiving general anesthesia. The recordings obtained included ECG (300 Hz), capnometry (25 Hz), and PPG (100 Hz) signals. All signals were recorded with S/5 Collect software (Datex-Ohmeda, Finland) using a sampling frequency of 300 Hz (PPG and capnometry with lower sampling rates were automatically up-sampled). The dataset including the annotation is available for download[1]. For this study, 132 2-min long data segments were randomly selected. A expert independently annotated each beat in the PPG using the CapnoBase Signal Evaluation Tool [13]. The expert also labeled the beginning and end of all visual artifacts in the PPG waveforms.

The algorithm was compared to the algorithm presented by [6] (CSL Reference algorithm). Two pulse oximetry recordings (pox1 and pox2) were provided by the Complex System Laboratory (CSL Benchmark dataset) and are available online[2]. The data were obtained from two pediatric cases in the pediatric intensive care unit. PPG was sampled at 125 Hz, band-pass filtered and auto-scaled. The CSL dataset contained manual beat annotations from two independent experts and the automatic annotation from the CSL Reference algorithm. The annotations of the expert with identification "DT" were chosen as reference beats for this work. Since

[1] http://www.CapnoBase.org
[2] http://bsp.pdx.edu/Data/

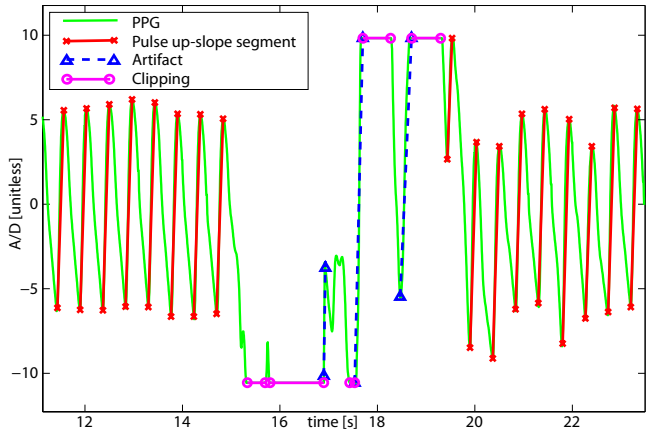

Fig. 2. Example output of the line segmentation algorithm. Up-slopes adjacent to clipping are automatically labeled as artifacts.

the CSL Benchmark dataset did not contain annotations for artifacts, the same independent expert that was annotating the CB dataset also labeled the CSL dataset for visual artifacts.

Algorithm implementation, data processing and statistical analysis were all performed using the Matlab software framework (Mathworks Inc, Natick, USA).

A. Performance Assessment

A beat-to-beat comparison between reference beat annotation and algorithm output was performed to assess the performance of the algorithm. The beats were considered to match if they were within an acceptance interval of 0.03 s. A learning period of 10 s was applied and the peaks falling in this period were not compared. The results were displayed in a confusion matrix. In addition, sensitivity (Se, percentage of correctly detected beats) and positive predictive value ($+P$, percentage of detected beats that were labeled as such) were calculated such that:

$$Se = \frac{TP}{TP + FN} \quad (1)$$

$$+P = \frac{TP}{TP + FP}, \quad (2)$$

where TP is the number of true positives, FN the number of false negatives, and FP the number of false positives.

IV. Results

A total of 15819 beats in the CSL dataset were analyzed by the algorithms. The line segmentation algorithm ($Se = 98.93$) was less sensitive than the CSL Reference algorithm ($Se = 99.81$) in detecting regular pulses because 131 beats were mistakenly labeled as artifacts (Table I). This is less than 0.09% of the analyzed beats. The number of beats labeled as normal that were artifact beats was reduced by the line segmentation algorithm to 57% and the number of beats labeled as normal beats that did not exist was reduced to 15.7% of the mislabeled beats from the CSL Reference algorithm (Table II), resulting in significant higher $+P$ for the segmentation algorithm. The number of missed pulses (artifact and normal) was very comparable.

TABLE I

PULSE DETECTION CONFUSION MATRIX OF THE IMS ALGORITHM ON THE CSL BENCHMARK DATASET

		Expert Annotation			+P [%]
		Regular Pulse	Artifact	None	
IMS Algorithm	Regular	14745	453	53	96.68
	Artifact	131	317	212	
	None	29	144	-	
Se [%]		98.93			

TABLE II

PULSE DETECTION CONFUSION MATRIX OF CSL REFERENCE ALGORITHM ON THE CSL BENCHMARK DATASET

		Expert Annotation			+P [%]
		Regular Pulse	Artifact	None	
CSL Algorithm	Regular	14877	782	336	93.01
	Artifact	-	-	-	
	None	28	132	-	
Se [%]		99.81			

V. DISCUSSION

We have presented a new algorithm for segmentation of PPG waveform into pulses and the automatic classification of artifacts. The IMS algorithm is iterative and can be easily implemented for real-time applications. It operates in the time-domain only and can be configured with a single parameter m which adjusts the segment size. The IMS algorithm computes faster and is less sensitive to noise with larger m, but the pulse peak detection is less precise in temporal space.

A comparison with the CSL Reference algorithm [6] shows comparable performance in detecting normal pulses (Table I and II). Since the CSL Reference algorithm was not designed for labeling artifacts a direct comparison for this task cannot be made. Whereas the CSL experts only annotated peaks that were clearly identifiable as such (a clipped pulse peak would not be marked as peak, but a pulse with a clipped base was marked), the third expert was more conservative and marked all artifact zones. As a result, there were artifact zones with no CSL labeled peaks or with labeled peaks that are visually regular, but were too close to an artifact. Consequently, the automated algorithm detected a significant number of peaks that were not present in the reference annotation. Since the algorithm output will be used for further high-level trend processing, such as respiratory rate extraction, signal quality estimation and heart rate variability calculation, a conservative artifact recognition (over-detection of artifacts) is desirable and has been used in the implementation.

The superiority of the line segmentation algorithm can be observed in that the majority of the mislabeled peaks (212) were correctly identified as artifacts. Overall, significantly fewer FP were obtained (506 vs. 1118). This always comes with a cost of reducing Se. The reduction of over-detected regular beats is more desirable than of over-detected artifacts. Therefore, we will aim to improve the artifact detection in this direction to further reduce the number of FP.

A limitation of this study was that, despite the large size of the CSL dataset, it only contained a limited number of PPG morphologies. For example, only few beats with dicrotic notches were present. Further benchmarking with a broader range of datasets that include adult recordings is required.

We are currently working towards a real-time implementation of the IMS algorithm into the Phone Oximeter platform [3], which will allow us to assess computational efficiency. With the Phone Oximeter we aim to provide a mobile, low-cost monitoring solution for pneumonia and other global diseases.

ACKNOWLEDGMENT

The authors would like to express their gratitude to Erin Cooke for her expertise in annotating the datasets and Joanne Lim for her helpful feedback on versions of this manuscript.

REFERENCES

[1] K. H. Shelley, "Photoplethysmography: beyond the calculation of arterial oxygen saturation and heart rate." *Anesthesia and analgesia*, vol. 105, no. 6 Suppl, pp. S31–6, 2007.

[2] P. D. Mannheimer, "The light-tissue interaction of pulse oximetry." *Anesthesia and analgesia*, vol. 105, no. 6 Suppl, pp. S10–7, 2007.

[3] W. Karlen, G. Dumont, C. Petersen, J. Gow, J. Lim, J. Sleiman, and J. M. Ansermino, "Human-centered Phone Oximeter Interface Design for the Operating Room," in *HEALTHINF 2011 - Proceedings of the International Conference on Health Informatics*, V. Traver, A. Fred, J. Filipe, and H. Gamboa, Eds. Rome: SciTePress, 2011, pp. 433–8.

[4] J. Weng, Z. Ye, and J. Weng, "An Improved Pre-processing Approach for Photoplethysmographic Signal." in *Annual International Conference of the IEEE Engineering in Medicine and Biology Society.* IEEE, Jan. 2005, pp. 41–4.

[5] U. Farooq, D.-G. Jang, J.-H. Park, and S.-H. Park, "PPG delineator for real-time ubiquitous applications." in *Annual International Conference of the IEEE Engineering in Medicine and Biology Society.* IEEE, Jan. 2010, pp. 4582–5.

[6] M. Aboy, J. McNames, T. Thong, D. Tsunami, M. S. Ellenby, and B. Goldstein, "An automatic beat detection algorithm for pressure signals." *IEEE Transactions on Biomedical Engineering*, vol. 52, no. 10, pp. 1662–70, 2005.

[7] W. Karlen, C. Petersen, J. Gow, J. M. Ansermino, and G. Dumont, "Photoplethysmogram Processing Using An Adaptive Single Frequency Phase Vocoder Algorithm," in *BIOSTEC 2011, CCIS 273*, A. Fred, J. Filipe, and H. Gamboa, Eds. Berlin Heidelberg: Springer-Verlag, 2012, pp. 31–42.

[8] J. A. Sukor, S. J. Redmond, and N. H. Lovell, "Signal quality measures for pulse oximetry through waveform morphology analysis." *Physiological measurement*, vol. 32, no. 3, pp. 369–84, 2011.

[9] B. S. Kim and S. K. Yoo, "Motion Artifact Reduction in Photoplethysmography Using Independent Component Analysis," *IEEE Transactions on Biomedical Engineering*, vol. 53, no. 3, pp. 2001–3, 2006.

[10] G. A. Borges and M.-J. Aldon, "Line Extraction in 2D Range Images for Mobile Robotics," *Journal of Intelligent and Robotic Systems*, vol. 40, no. 3, pp. 267–97, 2004.

[11] J. Vandorpe, H. Van Brussel, and H. Xu, "Exact dynamic map building for a mobile robot using geometrical primitives produced by a 2D range finder," in *Proceedings of the IEEE International Conference on Robotics and Automation*, Minneapolis, USA, 1996, pp. 901–9.

[12] H. Vullings, M. Verhaegen, and H. Verbruggen, "ECG segmentation using time-warping," in *Lecture notes in computer science*. Berlin/Heidelberg: Springer, 1997, pp. 275–86.

[13] W. Karlen, M. Turner, E. Cooke, G. Dumont, and J. M. Ansermino, "CapnoBase: Signal database and tools to collect, share and annotate respiratory signals," in *Annual Meeting of the Society for Technology in Anesthesia (STA)*, West Palm Beach, 2010, p. 25.